LAWRENCE
LIVERMORE
NATIONAL
LABORATORY

UCRL-PROC-227585

Bubble Counts for Rayleigh-Taylor Instability Using Image Analysis

P. L. Miller, A. G. Gezahegne, A. W. Cook, W. H. Cabot, C. Kamath

January 30, 2007

International Workshop on the Physics of Compressible Turbulent Mixing
Paris, France
July 17, 2006 through July 21, 2006

e-mail: pmiller@llnl.gov

Bubble Counts for Rayleigh-Taylor Instability Using Image Analysis

Paul L. MILLER[1], Abel GEZAHEGNE[1], Andrew COOK[1], William CABOT[1], and Chandrika KAMATH[1]

[1]*Lawrence Livermore National Laboratory*

Abstract: We describe the use of image analysis to count bubbles in 3-D, large-scale, LES [1] and DNS [2] of the Rayleigh-Taylor instability. We analyze these massive datasets by first converting the 3-D data to 2-D, then counting the bubbles in the 2-D data. Our plots for the bubble count indicate there are four distinct regimes in the process of the mixing of the two fluids. We also show that our results are relatively insensitive to the choice of parameters in our analysis algorithms.

1 BUBBLE-IDENTIFICATION ALGORITHM

The three-dimensional data from the simulations are converted through a series of steps to two-dimensional data for analysis. A region-growing approach is first used to define the mixing region from the density field. The data volume is then processed to produce a "top-down" image of the height of the top surface of the three-dimensional mixing region defined by the region-growing method. To locate bubble structures in the surface depicted in the height map, the magnitude of the X-Y velocity is computed, and localized nodes of zero X-Y velocity magnitude are used to identify the tips of bubbles. See Figs. 1.1 and 1.2.

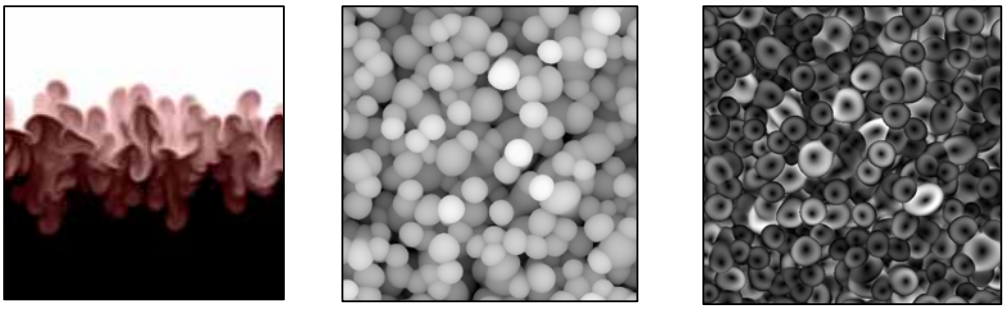

(a) **(b)** **(c)**

Fig. 1.1. DNS at $t / \tau = 6.25$. Only 1/36 of the area of the data is displayed. (a) 2-D slice of density, where the gray regions are identified by the 3-D region-growing method. (b) The height of the bubbles as seen in the top view obtained from 3-D region growing. (c) Magnitude of the X-Y velocity at the bubble boundary.

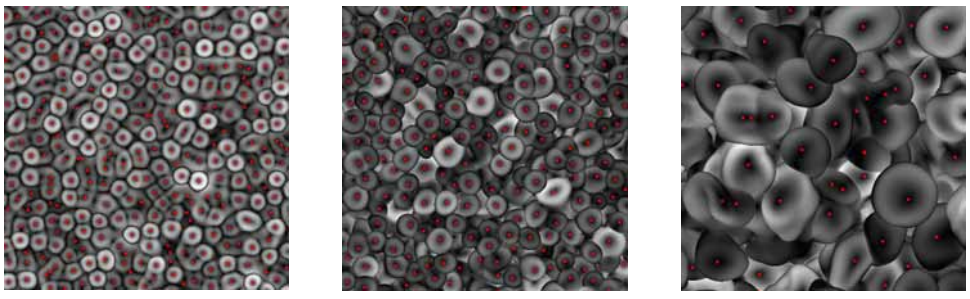

(a) **(b)** **(c)**

Fig. 1.2. Sub-images from the DNS, with the bubble tips identified, for t / τ of (a) 2.25, (b) 5.625, and (c) 14. A bubble tip is the centroid of a region where both the magnitude of the X-Y velocity and the height variation are small. Only 1/36 of the area of the data is displayed.

2 SENSITIVITY TO THRESHOLD

The method we employ to determine the location of bubble structures is necessarily subjective. We used visualization to verify the results from the algorithms as they were developed and refined, and took the approach that a bubble is a structure that manifests itself near the top region of the mixing layer, has a characteristic domed feature, and is something that a person viewing an image can recognize intuitively. These assumptions work well at the early times in the flow development, but are strained at late time when the flow morphology becomes quite complicated.

We explored the dependence of the final bubble counts on the threshold used in the region-growing step. For a subset of simulation times, the threshold was varied and the resulting bubble tips on the top-down images were judged by eye for whether the result was consistent with what our eye discerned in the structure. Upper and lower bounds were determined, and the dependence of the upper and lower bounds on the final bubble counts was determined (Figs. 2.1 and 2.2). The differences resulting from the extremes of the thresholds are observed to be relatively small when considering the slopes of the bubble count curves. For the primary analysis, a logarithmic function was constructed that represented a reasonable range of threshold values. The increase in the threshold with time is reflective of the varying impact of diffusion on the bubble front.

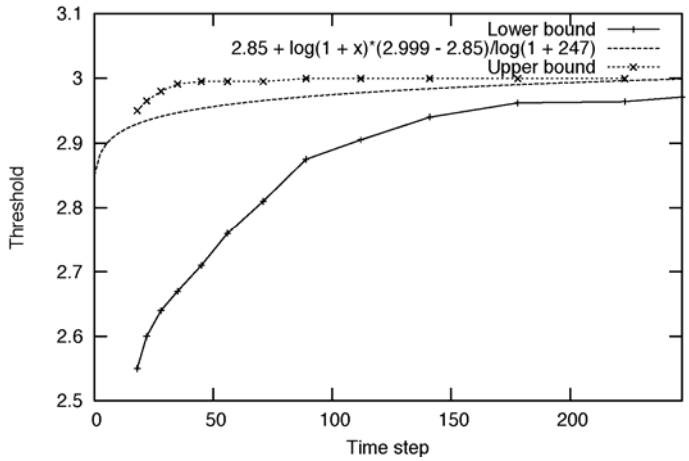

Fig. 2.1. Empirical range of thresholds observed to result in similar bubble identification (DNS).

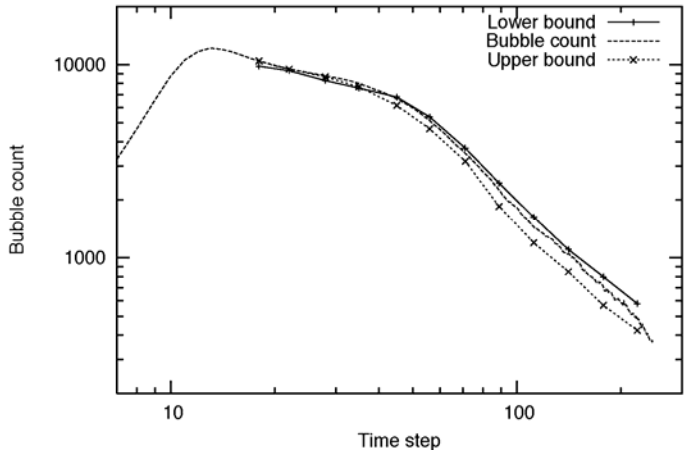

Fig. 2.2. The number of bubbles identified using the extreme thresholds in Fig. 2.1, as well as the result using the intermediate function-defined threshold values.

3 BUBBLE COUNTS

The bubble-identification algorithm was used to analyze data from two large-scale numerical simulations of the Rayleigh-Taylor instability, a Large-Eddy Simulation (LES) [1] and a Direct Numerical Simulation (DNS) [2]. The results are displayed in Figs. 3.1 and 3.2. Using log-log scales accentuates possible power-law scaling of the bubble count vs. nondimensional time (defined in [1]). Note that the log scales over-emphasize very early times. Also, the absolute value of the bubble count scale is arbitrary, simply reflecting the size of the analyzed domain.

Four regions emerge exhibiting different power-law behaviors, as indicated by the included line fits. The fit parameters are listed as measures of the curve slopes. The four regions are reminiscent of behavior observed previously [1] in other statistics of the mixing layer, such as the mixedness parameter and the growth rate. Roughly speaking, the four regions correspond to, from left to right, (1) early independent bubble growth, (2) nonlinear interactions between the growing structures, (3) a transition, and (4) fully turbulent regime. The more accentuated bump in the LES results (shallower region 3 slope) is not entirely understood, but may be related to a difference in effective Schmidt numbers between the two cases. Note the slopes do not drop below -2.28.

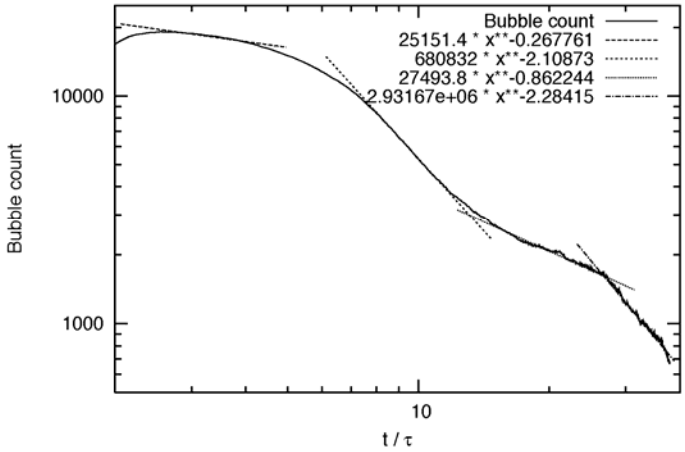

Fig. 3.1. Bubble counts for the LES, 1152^3 grid, 759 time steps, 30 terabytes of data.

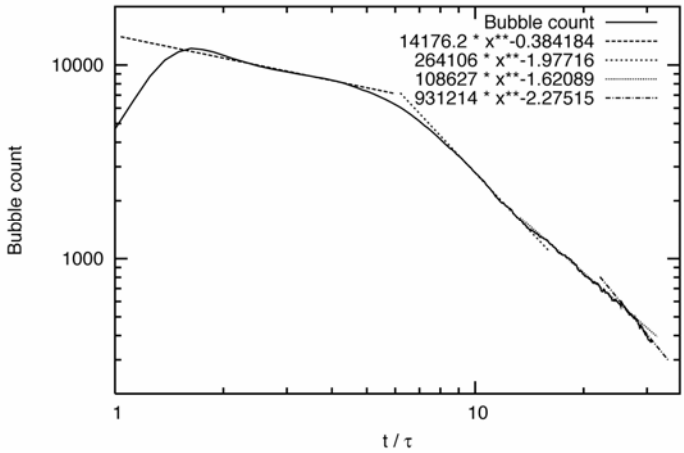

Fig. 3.2. Bubble counts for the DNS, 3072^3 grid, 248 time steps, 80 terabytes of data.

4 SUMMARY

In conclusion, we have developed a method for the identification of bubble structures in simulations of Rayleigh-Taylor instability, and applied the method to count bubbles in two large-scale data sets. We investigated the sensitivity of the results to the use of a subjective threshold, and found it has little influence on the power-law behavior of the bubble counts. Likewise, there are some differences in details, but the general conclusions hold for both the LES and the DNS datasets.

The log-log plots of bubble counts vs. nondimensional time exhibit four distinct regions. These regions correspond to qualitatively different bubble behavior. At the earliest times, the bubbles are very distinct and grow in a quasi-independent manner. Subsequently, the bubbles begin to interact, develop mushroom-cap rollups, and their stems begin to tilt and then intertwine with neighboring bubbles. The pattern soon becomes much more complex, and then undergoes a transition to a fully turbulent state. At the latest times, the mixing layer boundary has a wide spectrum of length scales represented in its structure, with bumps upon bumps, and a simplified concept of an idealized bubble becomes increasingly questionable.

The power-law scaling of these bubble counts has implications for bubble-based models of Rayleigh-Taylor instability. In particular, if the bubbles "tile" the area, then the number of bubbles should scale like the inverse of the square of the bubble radius. If it is further assumed that the characteristic bubble radius scales proportional to the layer width, and the mixing layer width scales like t^2, then the number of bubbles should be proportional to t^{-4}, i.e., a slope of -4 on the log-log plots of bubble count vs. time. Likewise, alternative scalings of the bubble radius will produce other power laws.

Our results do not exhibit slopes nearly as negative as -4, so we conclude that the destruction of bubbles (by whatever means, such as merging or competition) is slower than suggested by a bubble radius proportional to the layer width.

We have employed another analysis approach to the bubble-counting problem, with similar findings, that appears elsewhere in this Proceedings [3].

This work was performed under the auspices of the U.S. Department of Energy by the University of California Lawrence Livermore National laboratory under contract No. W-7405-Eng-48.

REFERENCES

[1] Cook et al., *The mixing transition in Rayleigh-Taylor instability*, JFM **511** (2004), 333 - 362.
[2] Cabot and Cook, *Reynolds number effects on Rayleigh-Taylor instability with possible implications for type-1a supernovae*, Nature Physics **2** (2006), 562 - 568.
[3] Miller, et al., *Application of Morse Theory to Analysis of Rayleigh-Taylor Topology*, elsewhere in this Proceedings.